Loss-of-Function Mutations in *LGI4*, a Secreted Ligand Involved in Schwann Cell Myelination, Are Responsible for Arthrogryposis Multiplex Congenita

Shifeng Xue,[1,2,17] Jérôme Maluenda,[3,17] Florent Marguet,[4,5,17] Mohammad Shboul,[1] Loïc Quevarec,[3] Carine Bonnard,[1] Alvin Yu Jin Ng,[2] Sumanty Tohari,[2] Thong Teck Tan,[1] Mung Kei Kong,[1] Kristin G. Monaghan,[6] Megan T. Cho,[6] Carly E. Siskind,[7] Jacinda B. Sampson,[7] Carolina Tesi Rocha,[7] Fawaz Alkazaleh,[8] Marie Gonzales,[9] Luc Rigonnot,[10] Sandra Whalen,[9] Marta Gut,[11,12] Ivo Gut,[11,12] Martine Bucourt,[13] Byrappa Venkatesh,[2,15] Annie Laquerrière,[4,5] Bruno Reversade,[1,2,14,15,16,18,*] and Judith Melki[3,18,*]

Arthrogryposis multiplex congenita (AMC) is a developmental condition characterized by multiple joint contractures resulting from reduced or absent fetal movements. Through genetic mapping of disease loci and whole-exome sequencing in four unrelated multiplex families presenting with severe AMC, we identified biallelic loss-of-function mutations in *LGI4* (leucine-rich glioma-inactivated 4). LGI4 is a ligand secreted by Schwann cells that regulates peripheral nerve myelination via its cognate receptor ADAM22 expressed by neurons. Immunolabeling experiments and transmission electron microscopy of the sciatic nerve from one of the affected individuals revealed a lack of myelin. Functional tests using affected individual-derived iPSCs showed that these germline mutations caused aberrant splicing of the endogenous *LGI4* transcript and in a cell-based assay impaired the secretion of truncated LGI4 protein. This is consistent with previous studies reporting arthrogryposis in *Lgi4*-deficient mice due to peripheral hypomyelination. This study adds to the recent reports implicating defective axoglial function as a key cause of AMC.

Arthrogryposis multiplex congenita (AMC) has an overall incidence of 1 in 3,000.[1,2] Non-syndromic or isolated AMCs are the direct consequence of reduced fetal movements that may lead, in addition to AMC, to pterygia, pulmonary hypoplasia, diaphragmatic defect, or cleft palate. Non-syndromic AMCs are genetically heterogeneous and include a large spectrum of diseases that arise as a result of mutations in genes encoding components required for the formation or the function of neuromuscular junctions, skeletal muscle, survival of motor neurons, or myelination of peripheral nerve.[3] However, many affected individuals remain without a genetic diagnosis, suggesting the involvement of other pathogenic mechanisms. Here, we further explored genetic alterations in a group of genetically undiagnosed AMCs.

The parents of all affected individuals provided written informed consent for pathological examinations and genetic analyses of their affected children or fetuses and themselves in accordance with the ethical standards of our institutional review boards. In family 1, two affected fetuses were born to consanguineous healthy parents. Based on ultrasound examination, the first male fetus displayed from 26 weeks of gestation (w.g.) a reduced mobility associated with right club foot, camptodactyly of left hand, and adduction of right thumb. These data were confirmed at 30 w.g. and the pregnancy was terminated at 33 w.g. at the request of the parents. Karyotype, *SMN1* (MIM: 600354), *DMPK* (MIM: 605377) analyses were normal. Postmortem examination confirmed distal arthrogryposis. Histological examination of the spinal cord was normal. For the second male fetus, ultrasound examination was normal at 13 w.g. and at 23 w.g. an almost identical phenotype characterized by camptodactyly of both hands associated with adduction of thumbs, right club foot, flexion of knees, and retrognathia was observed. The pregnancy was terminated at 26 w.g. at the request of the parents. Postmortem examination confirmed arthrogryposis. Genetic mapping of disease loci was carried out using Affymetrix GeneChip Human Mapping 250K SNP microarray. Multipoint linkage analysis of SNP data was performed using the Alohomora[4] and Merlin softwares.[5] Whole-exome sequencing (WES) was performed from DNA of the index

[1]Institute of Medical Biology, A*STAR, Singapore 138648, Singapore; [2]Institute of Molecular and Cell Biology, A*STAR, Singapore 138673, Singapore; [3]Institut National de la Santé et de la Recherche Médicale (Inserm) UMR-1169, Université Paris Sud, Le Kremlin Bicêtre 94276, France; [4]Pathology Laboratory, Rouen University Hospital, Rouen 76000, France; [5]Normandie Univ, UNIROUEN, INSERM, CHU Rouen, Laboratoire NeoVasc ERI28, Rouen 76000, France; [6]GeneDx, Gaithersburg, MD 20877, USA; [7]Stanford University, Stanford, CA 94304, USA; [8]Department of Obstetrics and Gynecology, University of Jordan, Amman 19241, Jordan; [9]Département de Génétique Médicale, Hôpital Trousseau, Université Pierre et Marie Curie, Paris 75571, France; [10]Service d'Obstétrique, Centre Hospitalier Sud-Francilien, Corbeil-Essonnes 91100, France; [11]CNAG-CRG, Centre for Genomic Regulation (CRG), Barcelona Institute of Science and Technology (BIST), Barcelona 08028, Spain; [12]Universitat Pompeu Fabra (UPF), Barcelona 08028, Spain; [13]Unité de fœtopathologie, Hôpitaux Universitaires Paris-Seine-Saint-Denis, Hôpital Jean Verdier, Bondy 93143, France; [14]Department of Medical Genetics, Koç University, School of Medicine (KUSoM), Istanbul 34450, Turkey; [15]Department of Paediatrics, School of Medicine, National University of Singapore, Singapore 119228, Singapore; [16]Amsterdam Reproduction & Development, Academic Medical Centre & VU University Medical Center, Amsterdam 1105 AZ, the Netherlands
[17]These authors contributed equally to this work
[18]These authors contributed equally to this work
*Correspondence: bruno@reversade.com (B.R.), judith.melki@inserm.fr (J.M.)
http://dx.doi.org/10.1016/j.ajhg.2017.02.006.

case subject (II.1) using the Exome Capture Agilent SureSelect XT V5 kit for library preparation and exome enrichment as previously described.[6] Sequencing was performed on a Genome Analyzer IIx Illumina instrument in paired-end mode with a read length of 2× 100 bp. Reads were aligned to the human reference genome sequence (UCSC hg19, NCBI build 37.3) via the BWA program.[7] Variants were selected using the SAMtools[8] then annotated using Annovar softwares.[9] Variants in coding regions (including non-synonymous and nonsense mutations), intron-exon junctions, or short coding insertions or deletions were selected when the minor allele frequency (MAF) was less than 0.0030. Combining genetic mapping of disease loci under the hypothesis of homozygosity by descent and WES, a homozygous missense mutation was identified in *LGI4* (GenBank: NM_139284.2; c.793G>A [p.Ala265Thr], Figures 1A and 1C). This mutation is predicted to be pathogenic with a high score (PolyPhen-2 score of 0.969).[10] This mutation is annotated in dbSNP146 (rs779232987) with a very low minor allele frequency (MAF) in ExAC database (0.000043). The mutation was confirmed by Sanger sequencing using primers flanking the mutation (Figure 1A and Table S1) in both affected fetuses and both parents were heterozygous carriers (Figure S2). Importantly, this mutation is located at the last nucleotide of exon 7 suggesting a potential effect on intron 7 splicing. Sequencing of RT-PCR product of *LGI4* cDNA from skeletal muscle RNA of affected individual II:2 revealed a retention of *LGI4* intron 7 leading to frameshift and premature stop codon (p.Ala265SerfsTer231, Figures 1B and S3, F1 in Figure 3E) establishing the deleterious effect of the c.793G>A mutation.

In family 2, two affected fetuses were born to unrelated healthy parents. Based on ultrasound examination at 23 w.g., the first female fetus displayed bilateral club foot associated with bilateral camptodactyly and atrophy of calves. Karyotype, *SMN1* (MIM: 600354), *DMPK* (MIM: 605377) analyses were normal. At 25 w.g., fetal akinesia was observed and associated with bilateral flexion of both feet and hands. The pregnancy was terminated at 27 w.g. at the request of the parents. Postmortem examination revealed microretrognathia, bilateral camptodactyly, adduction of thumbs, flexion of feet, pulmonary hypoplasia, and thin diaphragmatic cupolae (Figure S1). For the second female fetus, ultrasound examination was normal at 12 w.g. and at 18 w.g., a severe hypokinesia was observed associated with arthrogryposis. The pregnancy was terminated at 19 w.g. at the request of the parents. Postmortem examination revealed marked retrognathia associated with flexion of hands, camptodactyly, extension of elbows, flexion of feet, and diaphragmatic eventration. Combining genetic mapping of disease loci under the hypothesis of autosomal-recessive inheritance and WES, compound heterozygous mutations were identified in *LGI4* in the affected individuals of family 2 (Figures 1A and 1C). A heterozygous nonsense mutation (c.863G>A [p.Trp288*]) was identified. This variant was not annotated in the 1000 Genomes or ExAC Browser databases. The second mutation was a splicing mutation (c.793+5G>C). This mutation was not annotated in the 1000 Genomes or ExAC databases. Both mutations were confirmed by Sanger sequencing using primers flanking the mutations in both affected fetuses and were allelic (Figures 1A, S2 and Table S1). RT-PCR analysis of *LGI4* cDNA from skeletal muscle RNA of affected individual II:1 revealed two fragments (Figures 1B and S3). Sequencing of the upper one revealed a retention of *LGI4* intron 7 leading to frameshift and premature stop codon similar to that observed in family 1 (Figure S3) establishing the deleterious effect of the c.793+5G>C mutation on intron 7 splicing. Sequencing the lower fragment, similar in size to that found in control, revealed the nonsense mutation only (c.863G>A, Figures 1B and S3) indicating that these two RT-PCR fragments were allelic and that the splicing mutation leads to the absence of wild-type *LGI4* transcript. Immunolabeling experiments on paraffin-embedded sections confirmed the presence of numerous axons and Schwann cells, but myelin basic protein (MBP) immunoreactivity was absent (data not shown). The lack of myelin was observed on semi-thin sections stained with toluidine blue in the affected individual when compared to the sciatic nerve of an age-matched control (Figures 2A and 2B). Transmission electron microscopy confirmed the lack of myelinated fibers in the sciatic nerve of the affected individual when compared to an age-matched control case, in whom mean myelin sheath thickness was 0.31 ± 0.11 μm (Figures 2C and 2D), with a mean number of 36 myelinated axons per 5,000 μm^2. Quantitative analysis of axonal areas (3.32 ± 2.15 μm^2, n = 20) did not significantly differ from that of control (3.95 ± 2.01 μm^2, n = 30, Wilcoxon-Mann Witney test, p value = 0.2, Figure S3).

Family 3 is a consanguineous family from Jordan with three affected pregnancies. All affected fetuses presented with multiple joint contractures, affecting the wrists, elbows, hips, knees, and ankles (Figure S1). The first child was born but died within 2 weeks due to pulmonary hypoplasia and respiratory distress. The next two pregnancies were both terminated at 23 w.g. due to fetal death. DNA was obtained from II:3 and WES performed. The exome library was prepared on an ION OneTouch System and sequenced on an Ion Proton instrument (Life Technologies) using one ION PI chip. Sequence reads were aligned to the human GRCh37. Variants were filtered for common SNPs using the NCBI's "common and no known medical impacts" database (ClinVar), the Exome Aggregate Consortium (ExAC), the Exome Sequencing Project, and an in-house database of 158 sequenced samples. Under the hypothesis of autosomal-recessive inheritance, a homozygous splice-site mutation was identified in *LGI4* (c.1299+5G>T, Figures 1A and 1C). This mutation was not annotated in dbSNP or in the EXAC database. This private mutation was confirmed by Sanger sequencing and found to be homozygous in the proband, heterozygous in the parents, and absent in the unaffected sister (Figures

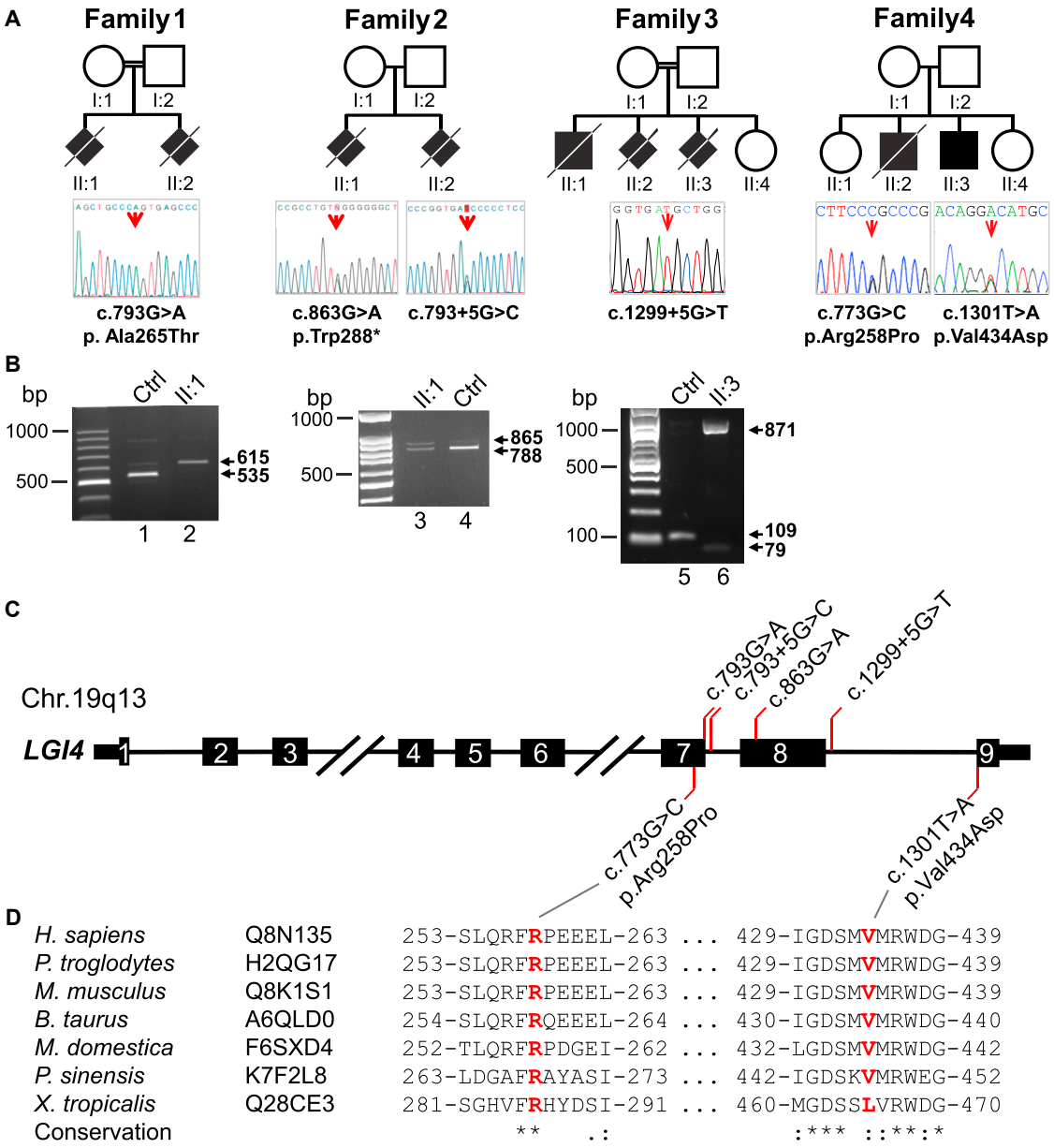

Figure 1. Germline Mutations in *LGI4* in Four AMC-Affected Families and Endogenous Transcript Analysis

(A) Pedigrees for AMC-affected families 1, 2, 3, and 4. Arrows indicate mutant nucleotide positions. The affected individuals carry either compound heterozygous (family 2 and 4) or homozygous (families 1 and 3) mutations. The nucleotide and amino acid changes are indicated with respect to the reference sequences (GenBank: NM_139284.2 and GenBank: NP_644813.1, respectively). Open symbols: unaffected; filled symbols: affected.

(B) cDNA analysis of *LGI4* in AMC-affected families. RT-PCR analysis was performed from RNA after reverse transcription by using random hexamers. Gel electrophoresis of RT-PCR products revealed abnormal fragments in affected individuals when compared to control (Ctrl) as the consequence of the spliced mutations. Sanger sequencing was performed from the RT-PCR products in control and affected individuals (Figure S2).

(C) Location of mutations in *LGI4*.

(D) Phylogenetic conservation of mutated residues in LGI4 vertebrate homologs. Accession numbers are from UniprotKB. Abbreviations are as follows: *M. domestica*, *Monodelphis domestica*; *P. sinensis*, *Pelodiscus sinensis*; asterisk (*) represents fully conserved residue; colon (:) represents residues with strongly similar properties; period (.) represents residues with weakly similar properties.

1A and S2). To test whether splicing of the endogenous *LGI4* transcript is affected in family 3, primary fibroblasts from fetus (II:3) were grown and reprogrammed into induced pluripotent stem cells (iPSCs) using the Cytotune 2 Sendai virus kit (Life Technologies). iPSCs were then differentiated into neural crest stem cells (NCSCs) as described previously (Figure 3A).[11] Murine *Lgi4* has been shown to be first expressed in vivo in neural crest cells of the developing peripheral nervous system.[12] In agreement with that, a marked increase in *LGI4* transcription was observed in control NCSCs compared to iPSCs (Figure 3B). Two clones of control and affected individual

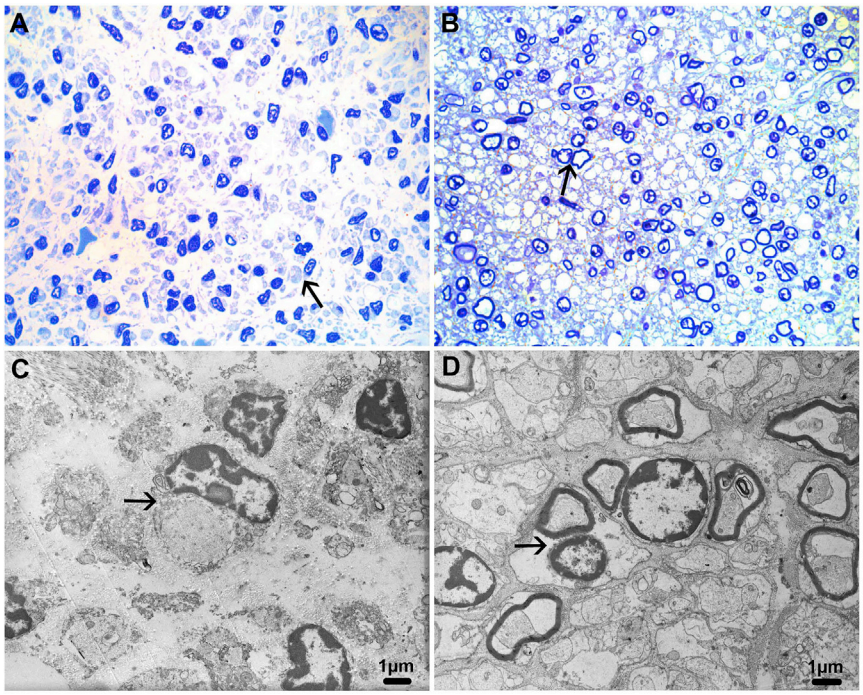

Figure 2. Morphological Characteristics of Nerve Lesions in the Affected Individual II:1 of Family 2 Carrying Deleterious *LGI4* Mutations

Tissue samples were fixed in a 2% glutaraldehyde fixative solution, post-fixed with osmium tetroxide, and embedded in resin epoxy. Semi-thin sections were stained with toluidine blue (A and B). Ultra-thin sections were contrasted with uranyl acetate and lead citrate and examined under a PHILIPS CM10 transmission electron microscope (C and D).

(A and B) Transverse semi-thin sections of the sciatic nerve of the affected fetus (A) displays no myelinated fibers when compared with an age-matched control case (B), where numerous myelinated fibers are observed (black arrows; original magnification 1,000).

(C and D) TEM transverse section of sciatic nerve of the affected fetus (C) confirms complete lack of myelinated fibers with normal endoneural cellularity mainly corresponding to Schwann cells (arrow), when compared to the control case, where numerous myelinated fibers (arrow) are observed (D). Scale bars represent 1 μm.

iPSCs were differentiated into NCSCs. By real-time quantitative RT-PCR, a 50% decrease in *LGI4* transcript levels was documented in affected individual-derived NSCSs relative to control NCSCs, suggesting nonsense-mediated decay of the endogenous transcript (Figure 3C). We next performed RT-PCR analysis of the mutant NCSC cDNA to detect possible splicing defects. Using primers spanning exons 7 to 8 and exons 7 to 9, multiple amplicons of varying size were cloned from the mutant cDNA and compared to the single wild-type amplicon (Figures 1B and 3D). Each amplicon (WT, F3a, F3b, and F3c) was gel-extracted, T-A cloned into pGEM-T vector (Promega), and sequenced. These correspond to three distinct aberrant splice forms: F3a retained intron 8, F3b used a cryptic splice site 47 nucleotides before the end of exon 8 to splice to exon 9, and F3c skipped exon 8 (Figures 3D and 3E). All three forms result in frameshifts and premature stop codons, establishing the deleterious effect of the c.1299+5G>T mutation. Consistently, using primers that detect only the wild-type transcript (Table S1), we performed quantitative PCR on control and mutant cDNA. The level of wild-type *LGI4* transcript fell to less than 5% of that in control cells (Figure 3F). Together, these results show that there is very little, if any, wild-type *LGI4* in these affected individuals.

Since the aberrantly spliced variants can be detected in the affected individual cells, albeit at a lower level, we sought to determine whether the resulting truncated proteins might retain functionality. The C-terminal of LGI4 contains seven epitempin (EPTP) repeats that fold into a β-propeller.[13] Any truncations that remove a portion of the EPTP repeats are likely to disrupt the β-propeller fold and affect the secretion of the protein. Wild-type *LGI4* cDNA or the various splice variants from families 1 and 3 were tagged with HA, cloned into expression vector pCS2, and transiently overexpressed into HEK293T cells. Cells were allowed to secrete proteins for 48 hr in serum-free medium before both the cells and the conditioned medium were harvested. An immunoprecipitation was performed from the medium using anti-HA magnetic beads (Pierce) to concentrate soluble LGI4. Western blot of the cell lysates showed a marked retention of mutant LGI4 proteins but little to no mutant protein in the conditioned medium. This was in contrast to wild-type LGI4 that was readily secreted (Figure 3G). This indicates that mutant truncated LGI4 are unable to be properly secreted and are retained in the cell.

Family 4 is a non-consanguineous family from Mexico with two affected children with AMC. The first male child was born with hypoxic ischemic encephalopathy, multiple contractures, respiratory distress, and pulmonary hypertension. He passed away within 2 hr of birth. The autopsy diagnoses included fetal akinesia sequence. The second affected child is now 6 years old. He was born at 40 weeks via emergency C-section after lack of heartbeat and breech presentation. He was born hypotonic, with contractures, and apneic, and was intubated until 4 months of age. Muscle biopsy suggested spinal anterior horn cell dysgenesis. Electromyographic study was consistent with a chronic neurogenic process. He had verbal developmental delay, having only 20 words at age of 4 years. Receptive language was better than spoken language. At 1 year, he developed tonic-clonic generalized and complex partial seizures. Brain MRI was normal. Dysmorphic features included prominent ears and a narrow forehead (Figure S1). He

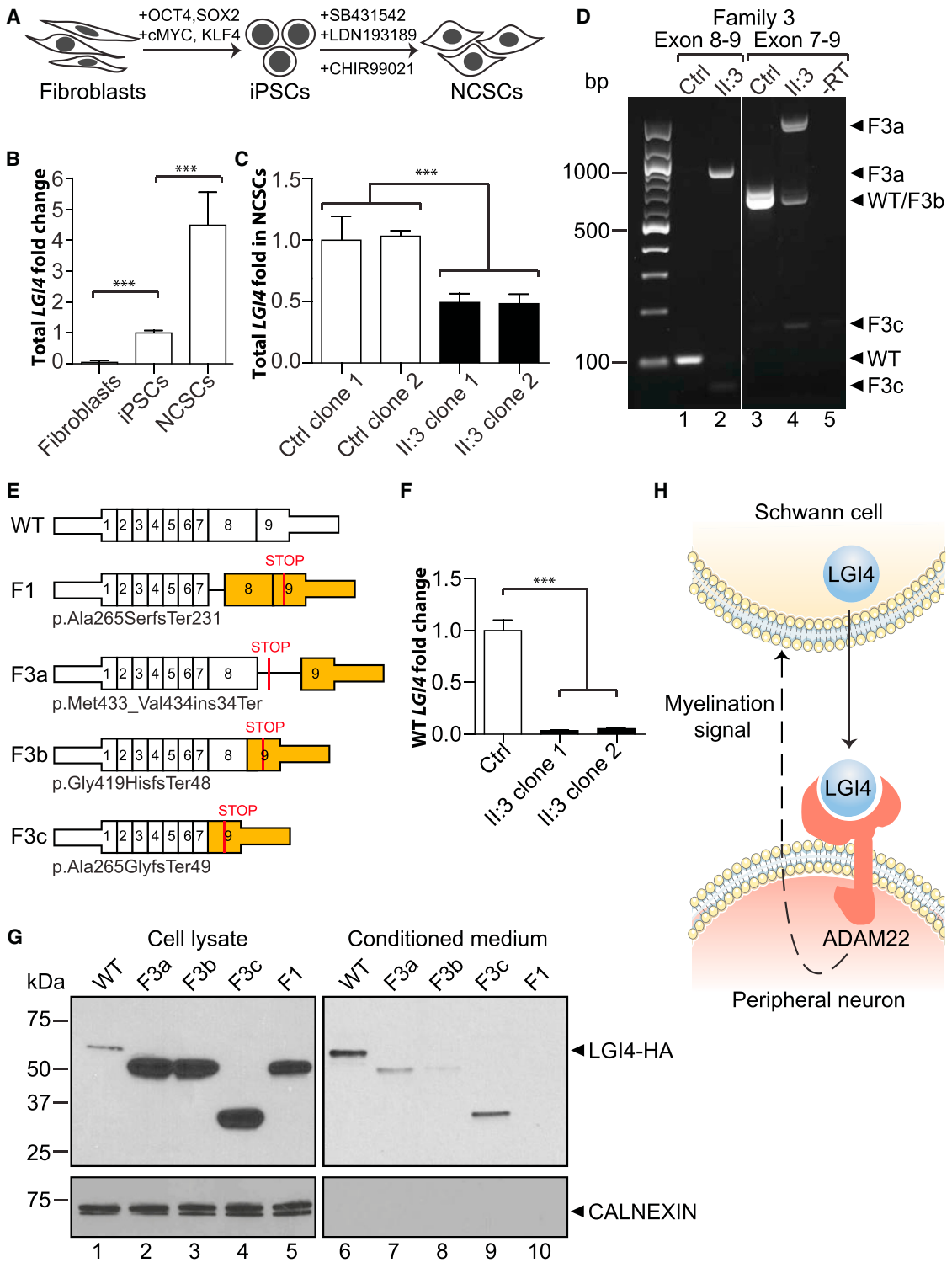

Figure 3. ***LGI4* Splice Mutations Reduce Endogenous mRNA Levels and Impair Secretion of Mutant LGI4**

(A) Primary dermal fibroblasts from control subject and affected individual II:3 of family 3 were reprogrammed to iPSCs and then differentiated to NCSCs using indicated transcription factors and small molecule inhibitors.

(B) Quantitative RT-PCR (qRT-PCR) analysis in fibroblasts, iPSCs, and NCSCs shows an upregulation of *LGI4* expression in NCSCs.

(C) qRT-PCR analysis shows a decrease in endogenous *LGI4* mRNA levels in affected individual-derived cells relative to control (Ctrl), suggestive of nonsense-mediated decay.

(D) RT-PCR analysis of NCSCs using primers spanning exons 8 and 9 (lanes 1, 2) and primers spanning exons 7 and 9 (lanes 3, 4, 5) shows that affected individual cells produce aberrantly spliced *LGI4* transcripts labeled F3a, F3b, and F3c.

(E) Schematic representation of the mRNA products from affected individual cells detected in (D) and Figure 1B. Frameshifted exons are colored orange and premature stop codons are denoted by red lines.

(legend continued on next page)

had bilateral esotropia, strabismus, ptosis, and decreased eye closure. The palate was very highly arched, with reduced mouth opening and dental crowding. He is hypotonic, with poor head control, low muscle bulk, and scoliosis. He has scapular winging with shoulder internal rotation, elbow hyperextension, pronation and ulnar deviation at wrists, with contractures in the hands with overlapping fusiform fingers (Figure S1). He is areflexic. DNA was obtained from II:3 and WES performed. Compound heterozygous mutations in *LGI4* were identified (c.773G>C; c.1301T>A) (Figures 1A and 1C). The first mutation (c.773G>C [p.Arg258Pro]) has been found in one individual in ExAC (allele frequency 9×10^{-6}) while the second mutation (c.1301T>A [p.Val434Asp]) has not been reported. The mutations were confirmed by Sanger sequencing of the proband and parents (Figure S2). Both variants occur on highly conserved residues and have PolyPhen-2 scores of 0.77 (p.Arg258Pro) and 0.98 (p.Val434Asp) (Figure 1D). These residues are located in the EPTP repeats of LGI4 and these variants may disrupt the β-propeller fold of the protein. Individual II:3 in this family has a milder phenotype than the affected individuals in other families probably because the missense mutations are less disruptive to the protein than the splice and nonsense mutations found in families 1–3. No functional experiments were performed due to the unavailability of affected individual cells.

The segregation and myelination of axons in the developing PNS result from complex cellular and molecular interactions between Schwann cells and axons. LGI4 is an important regulator of myelination in the PNS, and its dysfunction has been shown to be responsible for arthrogryposis and peripheral hypomyelination in *claw paw* mice (*clp*).[14] The *clp* mutation is a 225-bp insertion in the *Lgi4* locus.[15] *Lgi4* encodes a secreted and glycosylated leucine-rich repeat ligand specifically expressed in Schwann cells. The *clp* mutation affects *Lgi4* mRNA splicing, resulting in a mutant protein that is retained in cells. Lgi4 was therefore identified as a new component of Schwann cell signaling pathway(s) that controls axon segregation and myelin formation.[15] Consistently, gene-targeted mouse in which LacZ was knocked into the *Lgi4* locus through homologous recombination exhibits a defect in peripheral nerve myelination similar to, although more severe, than homozygous *clp* mice.[12]

Lgi4 has been shown to bind to the cell surface receptor Adam22, which is expressed by neurons.[15–18] Consistently, *Adam22*-deficient mice also exhibit defects in peripheral nerve myelination.[17] Moreover, using cell type-specific deletion of *Lgi4* or *Adam22* and heterotypic sensory neuron-Schwann cell cultures, it has been shown that Schwann cells are the principal source of Lgi4 and require binding to axonal Adam22 to drive myelin formation.[18] These data revealed a novel paracrine signaling pathway in peripheral nerve myelination in which Lgi4 synthesized and secreted by Schwann cells binds to axonal Adam22 to drive the differentiation and myelination of Schwann cells (Figure 3H). We show here that the germline mutations found in the affected individuals of families 1 and 3 cause a defect in LGI4 secretion which likely result in a defect in the crosstalk between Schwann cells and axons to initiate myelination. The mutations found in affected individuals of family 2, which consist in a nonsense mutation on one allele and intron 7 retention identical to that found in family 1 on the other allele, are expected to lead to similar defects. Consistently, an affected individual of this family showed a lack of myelin in the peripheral nerve. Lastly, we found compound heterozygous missense mutations in family 4. Based on the milder clinical presentation of the affected individual (II:3) in this family, these variants are likely hypomorphic compared to the splice-site or nonsense mutations found in the affected individuals of families 1–3 and causing lethal AMC.

Therefore, the biallelic mutations found in the affected individuals of these four families are likely to cause defective signaling of the LGI4 pathway similar to that observed in *Lgi4*-deficient mice. Recent data indicate that mutations of genes encoding CASPR-1[19] and gliomedin,[20] essential components of the nodes of Ranvier and paranodes, respectively, or proteins involved in myelination of Schwann cells such as ADCY6[19] and GPR126,[21] are responsible for severe human peripheral axoglial diseases, resulting in developmental defect of PNS, hypokinesia, and arthrogryposis. Here, we show that loss-of-function germline mutations of *LGI4* leads to a similar phenotype. As a secreted protein that is required for Schwann cell development and differentiation, LGI4 may be regarded as a novel therapeutic target to stimulate myelination in humans.

Supplemental Data

Supplemental Data include four figures and one table and can be found with this article online at http://dx.doi.org/10.1016/j.ajhg.2017.02.006.

Acknowledgments

We thank all families for partaking in this study. The authors would also like to thank Damien Gentil and members of their

(F) qRT-PCR using primers that detect correctly spliced transcripts only (WT) shows a dramatic reduction of WT *LGI4* transcripts in the affected individual cells of family 3.
(G) Different variants of *LGI4* from (E) were tagged with HA and transfected into HEK293T cells. Western blot using HA-HRP antibody (Sigma, H6533) shows that LGI4 mutants accumulate in the cell lysate whereas WT LGI4 is enriched in the conditioned media. This suggests that truncated LGI4 proteins fail to be properly secreted. Calnexin (Abcam, ab31290) was used as a loading control.
(H) LGI4 is secreted by Schwann cells and signals through its cognate receptor ADAM22 expressed on the surface of peripheral neurons. This signal transduction is believed to signal back to Schwann cells to induce myelination. ***$p < 0.001$.

team for technical assistance and fruitful discussions. This work was supported by a grant from the French Ministry of Health (PHRC 2010, AOM10181), the Association Française contre les Myopathies (AFM, DAJ1891), Agence Nationale pour la Recherche (HYPER-MND), University Paris Sud, and Inserm (to J. Melki) and a Strategic Positioning Fund on Genetic Orphan Diseases from the Biomedical Research Council, A*STAR, Singapore (to B.R.). K.G.M. and M.T.C. are employees of GeneDx.

Received: October 21, 2016
Accepted: February 16, 2017
Published: March 16, 2017

Web Resources

1000 Genomes, http://www.internationalgenome.org/
ANNOVAR, http://annovar.openbioinformatics.org/en/latest/
BLAST, http://blast.ncbi.nlm.nih.gov/Blast.cgi
ClinVar, ftp://ftp.ncbi.nlm.nih.gov/pub/clinvar/vcf_GRCh37/
dbSNP146, http://www.ncbi.nlm.nih.gov/snp
ExAC Browser, http://exac.broadinstitute.org/
GenBank, http://www.ncbi.nlm.nih.gov/genbank/
Human Splicing Finder, http://www.umd.be/HSF3/HSF.html
NHLBI Exome Sequencing Project (ESP) Exome Variant Server, http://evs.gs.washington.edu/EVS/
OMIM, http://www.omim.org/
PolyPhen-2, http://genetics.bwh.harvard.edu/pph2/
UniProt, http://www.uniprot.org/

References

1. Hall, J.G. (1985). Genetic aspects of arthrogryposis. Clin. Orthop. Relat. Res. (194), 44–53.
2. Fahy, M.J., and Hall, J.G. (1990). A retrospective study of pregnancy complications among 828 cases of arthrogryposis. Genet. Couns. *1*, 3–11.
3. Hall, J.G. (2014). Arthrogryposis (multiple congenital contractures): diagnostic approach to etiology, classification, genetics, and general principles. Eur. J. Med. Genet. *57*, 464–472.
4. Rüschendorf, F., and Nürnberg, P. (2005). ALOHOMORA: a tool for linkage analysis using 10K SNP array data. Bioinformatics *21*, 2123–2125.
5. Abecasis, G.R., Cherny, S.S., Cookson, W.O., and Cardon, L.R. (2002). Merlin--rapid analysis of dense genetic maps using sparse gene flow trees. Nat. Genet. *30*, 97–101.
6. Zhou, J., Tawk, M., Tiziano, F.D., Veillet, J., Bayes, M., Nolent, F., Garcia, V., Servidei, S., Bertini, E., Castro-Giner, F., et al. (2012). Spinal muscular atrophy associated with progressive myoclonic epilepsy is caused by mutations in ASAH1. Am. J. Hum. Genet. *91*, 5–14.
7. Li, H., and Durbin, R. (2009). Fast and accurate short read alignment with Burrows-Wheeler transform. Bioinformatics *25*, 1754–1760.
8. Li, H., Handsaker, B., Wysoker, A., Fennell, T., Ruan, J., Homer, N., Marth, G., Abecasis, G., Durbin, R.; and 1000 Genome Project Data Processing Subgroup (2009). The Sequence Alignment/Map format and SAMtools. Bioinformatics *25*, 2078–2079.
9. Wang, K., Li, M., and Hakonarson, H. (2010). ANNOVAR: functional annotation of genetic variants from high-throughput sequencing data. Nucleic Acids Res. *38*, e164.
10. Adzhubei, I.A., Schmidt, S., Peshkin, L., Ramensky, V.E., Gerasimova, A., Bork, P., Kondrashov, A.S., and Sunyaev, S.R. (2010). A method and server for predicting damaging missense mutations. Nat. Methods *7*, 248–249.
11. Mica, Y., Lee, G., Chambers, S.M., Tomishima, M.J., and Studer, L. (2013). Modeling neural crest induction, melanocyte specification, and disease-related pigmentation defects in hESCs and patient-specific iPSCs. Cell Rep. *3*, 1140–1152.
12. Nishino, J., Saunders, T.L., Sagane, K., and Morrison, S.J. (2010). Lgi4 promotes the proliferation and differentiation of glial lineage cells throughout the developing peripheral nervous system. J. Neurosci. *30*, 15228–15240.
13. Kegel, L., Aunin, E., Meijer, D., and Bermingham, J.R. (2013). LGI proteins in the nervous system. ASN Neuro *5*, 167–181.
14. Koszowski, A.G., Owens, G.C., and Levinson, S.R. (1998). The effect of the mouse mutation claw paw on myelination and nodal frequency in sciatic nerves. J. Neurosci. *18*, 5859–5868.
15. Bermingham, J.R., Jr., Shearin, H., Pennington, J., O'Moore, J., Jaegle, M., Driegen, S., van Zon, A., Darbas, A., Ozkaynak, E., Ryu, E.J., et al. (2006). The claw paw mutation reveals a role for Lgi4 in peripheral nerve development. Nat. Neurosci. *9*, 76–84.
16. Fukata, Y., Adesnik, H., Iwanaga, T., Bredt, D.S., Nicoll, R.A., and Fukata, M. (2006). Epilepsy-related ligand/receptor complex LGI1 and ADAM22 regulate synaptic transmission. Science *313*, 1792–1795.
17. Sagane, K., Ishihama, Y., and Sugimoto, H. (2008). LGI1 and LGI4 bind to ADAM22, ADAM23 and ADAM11. Int. J. Biol. Sci. *4*, 387–396.
18. Ozkaynak, E., Abello, G., Jaegle, M., van Berge, L., Hamer, D., Kegel, L., Driegen, S., Sagane, K., Bermingham, J.R., Jr., and Meijer, D. (2010). Adam22 is a major neuronal receptor for Lgi4-mediated Schwann cell signaling. J. Neurosci. *30*, 3857–3864.
19. Laquérriere, A., Maluenda, J., Camus, A., Fontenas, L., Dieterich, K., Nolent, F., Zhou, J., Monnier, N., Latour, P., Gentil, D., et al. (2014). Mutations in CNTNAP1 and ADCY6 are responsible for severe arthrogryposis multiplex congenita with axoglial defects. Hum. Mol. Genet. *23*, 2279–2289.
20. Maluenda, J., Manso, C., Quevarec, L., Vivanti, A., Marguet, F., Gonzales, M., Guimiot, F., Petit, F., Toutain, A., Whalen, S., et al. (2016). Mutations in *GLDN* encoding gliomedin, a critical component of nodes of Ranvier, are responsible for lethal arthrogryposis. Am. J. Hum. Genet. *99*, 928–933.
21. Ravenscroft, G., Nolent, F., Rajagopalan, S., Meireles, A.M., Paavola, K.J., Gaillard, D., Alanio, E., Buckland, M., Arbuckle, S., Krivanek, M., et al. (2015). Mutations of GPR126 are responsible for severe arthrogryposis multiplex congenita. Am. J. Hum. Genet. *96*, 955–961.